OAK RIDGE NATIONAL LABORATORY
OPERATED BY
UNION CARBIDE CORPORATION
NUCLEAR DIVISION

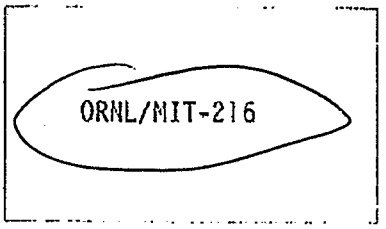

DATE: September 29, 1975

COPY NO.

SUBJECT: Cocurrent Three-Phase Fluidized Bed, Part 3

AUTHOR: S. Khosrowshahi, S.R. Bloxom, C. Guzman, and R.M. Schlapfer

Consultants: J.S. Watson and J.M. Begovich

ABSTRACT

The basic hydrodynamic variables of minimum fluidization and phase holdups were experimentally determined in a three-phase fluidized bed. Packings of 4x8 and 8x12 mesh alumina and 0.25-in. Plexiglas were fluidized by a cocurrent flow of air and water in 3- and 6-in.-diam Plexiglas columns. The holdups and minimum fluidization velocities were calculated from a pressure profile of the column. Correlations for the solid holdup as a function of the phase properties and operating parameters are presented.

Oak Ridge Station
School of Chemical Engineering Practice
Massachusetts Institute of Technology

Contents

1. SUMMARY

Applications of three-phase fluidized beds such as catalytic hydrogenation, coal liquefaction, and biochemical conversion require a better understanding of the design and operating characteristics of these contactors. A study was undertaken to correlate the hydrodynamic parameters important to the design of these beds.

The experimental apparatus consisted of two columns of 3- and 6-in.-ID, 0.25-in., spherical, Plexiglas beads, and 4x8 and 8x12 mesh alumina beads were fluidized with gas and liquid in the two columns. Pressure drop was measured for different flow rates, and the corresponding holdups were calculated from the equations defining the system. Incipient fluidization was determined from a plot of pressure drop as a function of liquid velocity at the point where the pressure drop becomes independent of liquid velocity. Correlations for the three holdups were attempted. The following equations were obtained for solid holdup:

$$1 - \varepsilon_S = 0.596\ Ca_G^{-0.0059 \pm 0.0042}\ Fr_L^{0.069 \pm 0.006}$$

$$1 - \varepsilon_S = 1.17\ Re_L^{0.231 \pm 0.009}\ Ar_L^{-0.157 \pm 0.005}$$

Liquid and gas holdups could not be correlated.

2. INTRODUCTION

2.1 Background

A three-phase fluidized bed is a bed of solid particles suspended by an upward cocurrent flow of gas and liquid. The principal application of these contactors is as catalytic reactors involving gas and liquid reactants and a solid catalyst. This application includes the hydrogenation of liquid petroleum fractions, the hydrogenation of unsaturated fats, and Fisher-Tropsch type processes. In coal liquefaction processes currently under development, the solid phase of the fluidized bed contains both a catalyst and a solid reactant. Knowledge of the flow behavior in a three-phase fluidized bed is essential to the analysis and design of such industrial operations.

2.2 Theory

When a fluid is passed upward through a bed of solid particles, pressure drop occurs. This pressure increases linearly with distance

through the bed of solids. The total pressure drop across the bed increases linearly with the fluid flow rates. At the minimum fluidization velocity the drag force exerted on the particles by the fluid exactly counterbalances the buoyant weight of solids. There is no further increase in pressure drop across the bed at velocities above minimum fluidization.

2.3 Previous Work

Kim et al. (5) studied the characteristics of two- and three-phase fluidized beds. Three-phase systems of water, air, and solids (gravel and glass) ranging in size from 3 to 6 mm were studied varying the superficial liquid velocity from 1.4 to 10.2 cm/sec and the superficial gas velocity from 0 to 26 cm/sec in a two-dimensional column (243.8 x 66 x 2.5 cm). The expanded bed height was measured and solid holdup was obtained from the bed height with Eq. (1). The gas and liquid holdups (ε_G and ε_L) were determined by simultaneous solution of Eqs. (2) and (3).

$$\varepsilon_S = M/\rho_S A H_B \tag{1}$$

$$\varepsilon_L + \varepsilon_G + \varepsilon_S = 1.0 \tag{2}$$

$$\Delta P = (\varepsilon_L \rho_L + \varepsilon_G \rho_G + \varepsilon_S \rho_S) g H_B \tag{3}$$

Kim also measured photographically the bubble diameter and velocity and reports two forms of three-phase fluidization: bed contraction on introduction of gas and bed expansion on introduction of gas. These two forms depend on a critical particle size, above which only bed expansion is observed. Kim found that for particles with densities of 2.5 gm/cm^3, fluidized by air and water, the critical diameter is 2.5 mm. In an extension of this investigation, Kim et al. (6) employed the same gas and solid phases but varied the viscosity from 1 to 70 cp with sugar and carboxymethyl cellulose solutions and varied the surface tension from 40 to 73 dynes/cm with acetone. Kim also performed experiments with 1-mm glass beads in the two-dimensional column varying superficial liquid velocity from 2.7 to 10.2 cm/sec and superficial gas velocity from 0.70 to 16.1 cm/sec. He obtained three correlations for three phase fluidized beds. For beds which initially expand on introduction of gas:

$$\varepsilon_L + \varepsilon_G = 1.4(Fr_L)^{0.170}(Ca_G)^{0.078} \tag{4}$$

For beds which initially contract on introduction of gas:

$$\varepsilon_L + \varepsilon_G = 1.301(Fr_L)^{0.128}(Ca_G)^{0.073}\, e^{0.031(V_L/V_G)\varepsilon_{L_2}} \tag{5}$$

where ε_{L_2} is liquid holdup from a two-phase (liquid-solid) fluidized bed given by:

$$\varepsilon_{L_2} = 1.353\ (Fr_L)^{0.206}\ (Re_L)^{-0.10} \tag{6}$$

For liquid holdup, Kim et al. proposed

$$\varepsilon_L = 1.504(Fr_L)^{0.234}\ (Fr_G)^{-0.086}\ (Re_L)^{-0.082}\ (Ca_G)^{0.092} \tag{7}$$

Dakshinamurty et al. (2) studied the fluidization characteristics of air-water-solids and air-kerosene-solids systems in a column 6-cm in diameter and 150-cm high varying the superficial gas velocity from 0.1 to 7.5 cm/sec and the superficial liquid velocity from 1 to 20 cm/sec. Several solids including rockwool shot, glass spheres, glass beads, iron shot, and sand ranging in density and diameter from 2.4 to 7.7 gm/cm^3 and from 0.1 to 0.7 cm, respectively, were fluidized. They reported a correlation for bed porosity in terms of the terminal velocity:

For $Re_t = \dfrac{\rho_L U_t D_p}{\mu_L} > 500$,

$$\varepsilon_L + \varepsilon_G = 2.65\left(\frac{U_L}{U_t}\right)^{0.6}\left(\frac{\mu_L U_G}{\sigma}\right)^{0.08} \tag{8}$$

For $Re_t < 500$,

$$\varepsilon_L + \varepsilon_G = 2.2\left(\frac{U_L}{U_t}\right)^{0.41}\left(\frac{\mu_L U_G}{\sigma}\right)^{0.08} \tag{9}$$

Østergaard and Michelsen (7) investigated the effect of gas and liquid velocities and particle size on gas holdup using a tracer technique. The experiments were carried out with water, air, and glass ballotini. The fluidization column of borosilicate tubing was 21.6-cm ID and 4.7 m long; the total height of the experimental section was 4.4 m. Flow rates of gas and liquid were measured by calibrated rotameters. The tracer materials were radioactive gamma-ray emitting isotopes: bromine-82 in the liquid phase (in the form of aqueous ammonium bromide solution) and argon-41 in the gas phase. Østergaard obtained a correlation for the gas holdup as a function of the superficial gas and liquid velocities:

$$\varepsilon_G = (2.50 \pm 0.05) \times 10^{-2}(0.193\ U_L)^{-0.16\pm0.02}(1.2\ U_G)^{1.05\pm0.03} \tag{10}$$

Burck et al. (1) performed experiments in a 3-in.-ID column varying gas and liquid superficial velocities. Burck studied three packings: 4x8 alumina, 8x12 alumina, and 0.25-in. Plexiglas beads and developed a correlation for solid holdup in terms of the minimum fluidization velocity.

$$\varepsilon_S = 0.51\left(\frac{U_L}{U_{L_{min}}}\right)^{-0.076\pm0.02} \tag{11}$$

Wen and Yu (8) studied liquid-solid fluidized beds of glass and steel balls, varying diameter from 0.08 to 0.25 cm and density from 2.36 to 7.84 gm/cm^3. Wen correlated his data with a large amount of literature data and obtained a correlation for bed porosity.

$$Ar_L \varepsilon_L^{4.7} = 18\, Re_L + 2.7\, Re_L^{1.687} \tag{12}$$

Ferguson et al. (4) performed experiments in 6-in.-ID and 3-in.-ID bubble columns varying gas and liquid superficial velocities. Ferguson obtained a correlation for gas holdup

$$\varepsilon_G = 0.322\left(\frac{\rho_L U_G^4}{g\sigma}\right)^{0.219} \tag{13}$$

2.4 Objectives

The objectives were to correlate the hydrodynamic variables of minimum fluidization velocities and phase holdups in a three phase fluidized bed over a range of operating conditions, and to recommend improvement in the experimental apparatus and to make suggestions for the continuation of this investigation.

2.5 Method of Attack

The hydrodynamic variables affecting the operation of three-phase fluidized beds were studied in two Plexiglas columns of 3- and 6-in. diameters. The pressure drop across the bed was monitored at a range of fluid velocities to determine the minimum fluidization velocities. The phase holdups were calculated from the bed height and pressure drop across the bed. For operating conditions where there is a well-defined bed height, the solid holdup was calculated from Eq. (1). The liquid and gas holdups were determined by the simultaneous solution of Eqs. (2) and (3). For flow rates where a definite bed height could not be determined, photographs were taken in an attempt to calculate the solid holdups.

To develop reasonable correlations for the solid, liquid, and gas holdups in the limit, the following criteria were established: (1) the correlation should approach known two-phase correlations as one of the phases vanishes, and (2) the sum of the holdups has to be unity. From previous investigations, the variables which were considered for correlating the phase holdups are:

$$\rho_S,\ \rho_L,\ \rho_G,\ U_L,\ U_G,\ \mu_L,\ \sigma,\ g,\ D_p$$

The dimensionless groups that were formed are consistent with those of previous investigators and are:

$$Re_L,\ Re_G,\ Ca_G,\ Fr_L,\ Fr_G,\ Ar_L$$

With these holdup criteria in mind and the above dimensionless groups, several correlations were attempted using a multivariable linear regression technique. The correlations were based on 105 experimental data points and 721 data points from the literature (2, 3, 5, 6, 7).

3. APPARATUS AND PROCEDURE

3.1 Apparatus

A flowsheet of the experimental apparatus is shown in Fig. 1. Three-phase fluidized beds were operated in two Plexiglas columns of 3- and 6-in.-ID. Water is pumped from two 55-gal feed tanks through a series of rotameters to the bottom of one of the columns where a screen acts as a liquid distributor. Similarly, air from an air line flows through a series of gas rotameters to a gas distributor located directly above the liquid distributor screen. The air and water flow cocurrently upwards through the column. The exit air is vented to atmosphere and the water overflows and is recirculated to the feed tanks. A series of water-filled manometers are located at intervals along both columns.

3.2 Procedure

Three packings were fluidized in the two columns: 4x8 and 8x12 mesh alumina beads and 0.25-in.-diam Plexiglas spheres. The alumina beads were pretreated with water to allow for adsorption in the porous material. The alumina was drained and sorted to eliminate broken particles. All packings were weighed, the densities determined by water displacement, and an average particle diameter determined by measurement with a micrometer. Initial

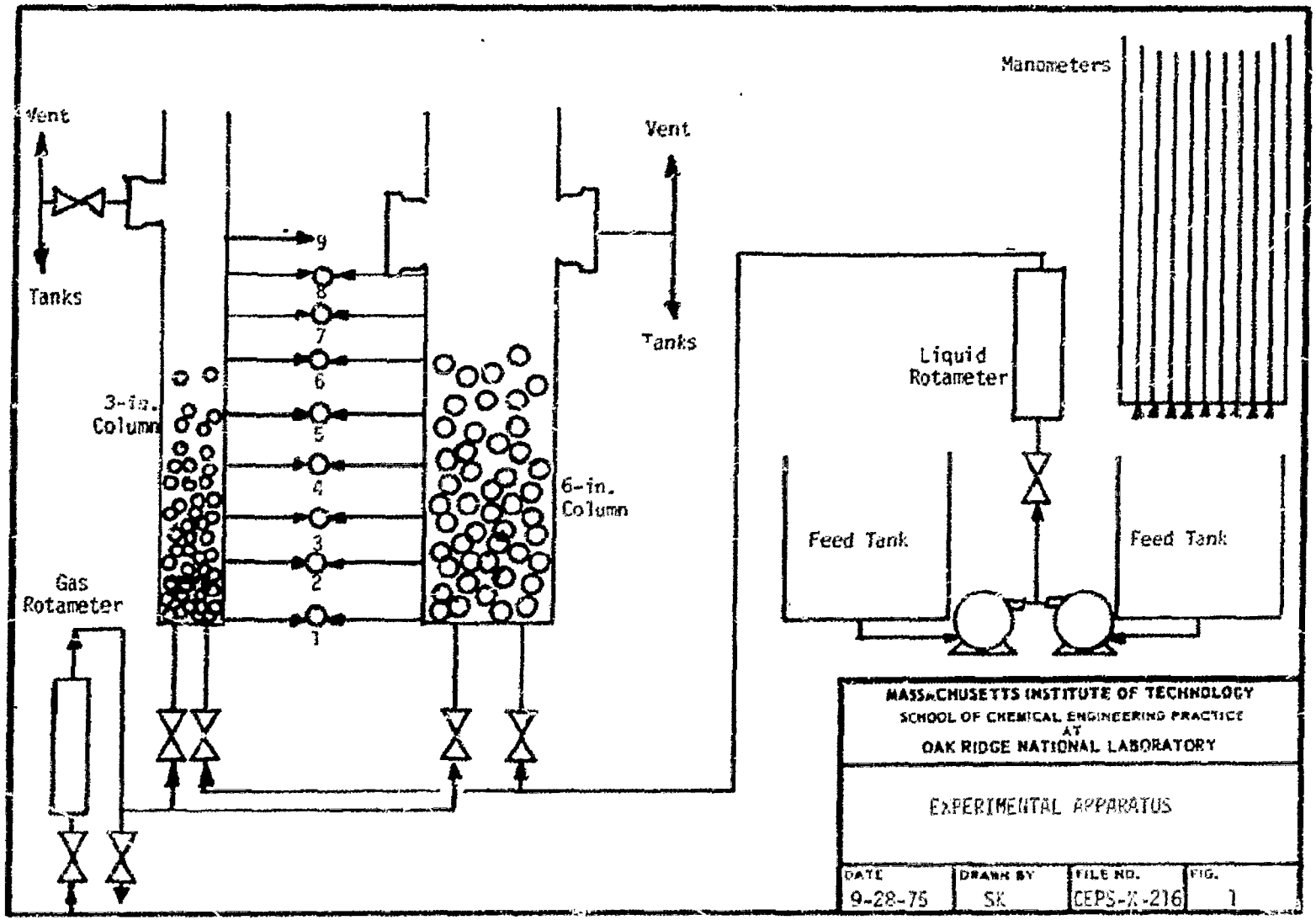
Manometers
Vent
Tanks
Vent
Tanks
9
8
7
6
5
4
3
2
1
3-in. Column
6-in. Column
Liquid Rotameter
Feed Tank
Feed Tank
Gas Rotameter
MASSACHUSETTS INSTITUTE OF TECHNOLOGY
SCHOOL OF CHEMICAL ENGINEERING PRACTICE
AT
OAK RIDGE NATIONAL LABORATORY
EXPERIMENTAL APPARATUS
DATE 9-28-75
DRAWN BY SK
FILE NO. CEPS-X-216
FIG. 1

readings of the manometers were taken, and the readings adjusted relative to the bottom manometer by the addition of a correction factor. This procedure corrects for elevation differences in the position of the manometer scales.

Gas was metered into the column at a specified superficial gas velocity. The liquid superficial velocity was varied over the range from 0 to 23 cm/sec. The pressure profile along the column was determined at each liquid velocity from the series of water manometers. The pressure drop due to flow was measured as the difference between the bottom manometer reading and each corrected manometer reading. The bed height occupied by solid particles and pressure drop across the bed were determined by a plot of pressure drop against distance up the column as shown in Fig. 2. Under some operating conditions, the points on this plot showed curvature near the maximum; in these cases a curve was fitted to the points around the maximum, and the bed height and pressure drop were taken at the apex of the curve. The values of pressure drop and bed height were substituted into Eqs. (1), (2), and (3) to calculate the phase holdups. A series of such measurements was made at several different liquid flow rates. The minimum fluidization velocity was determined by a plot of the pressure drop across the bed against the liquid superficial velocity. A typical minimum fluidization curve is shown in Fig. 3.

A photographic technique for the determination of solid holdup in regions of indefinite bed height was examined. Polaroid pictures of a Plexiglas packing consisting of a known ratio of black to clear particles were taken at intervals up the column. Equations (2) and (3) can then be applied over small intervals for the determination of holdups.

4. RESULTS AND DISCUSSION OF RESULTS

4.1 Pressure Drop

The reduced pressure drop through the bed as a function of superficial liquid velocity is shown in Fig. 4 for three superficial gas velocities with 8x12 mesh alumina in the 3-in. column. All pressure drop measurements were subject to $\pm$ 2 mm error in reading the manometer. The pressure drop increases with increasing liquid velocities below minimum fluidization. The minimum liquid fluidization velocities were determined as the points at which the pressure drops became independent of further increases in liquid velocities. At these points the beds are said to be fluidized. With increasing gas superficial velocities the fluidization points occurred at lower superficial liquid velocities and reduced pressure drops.

4.2 Minimum Gas and Liquid Fluidization Velocities

The minimum gas and liquid superficial velocities as a function of packing and column diameter are illustrated in Figs. 5 and 6. The weak

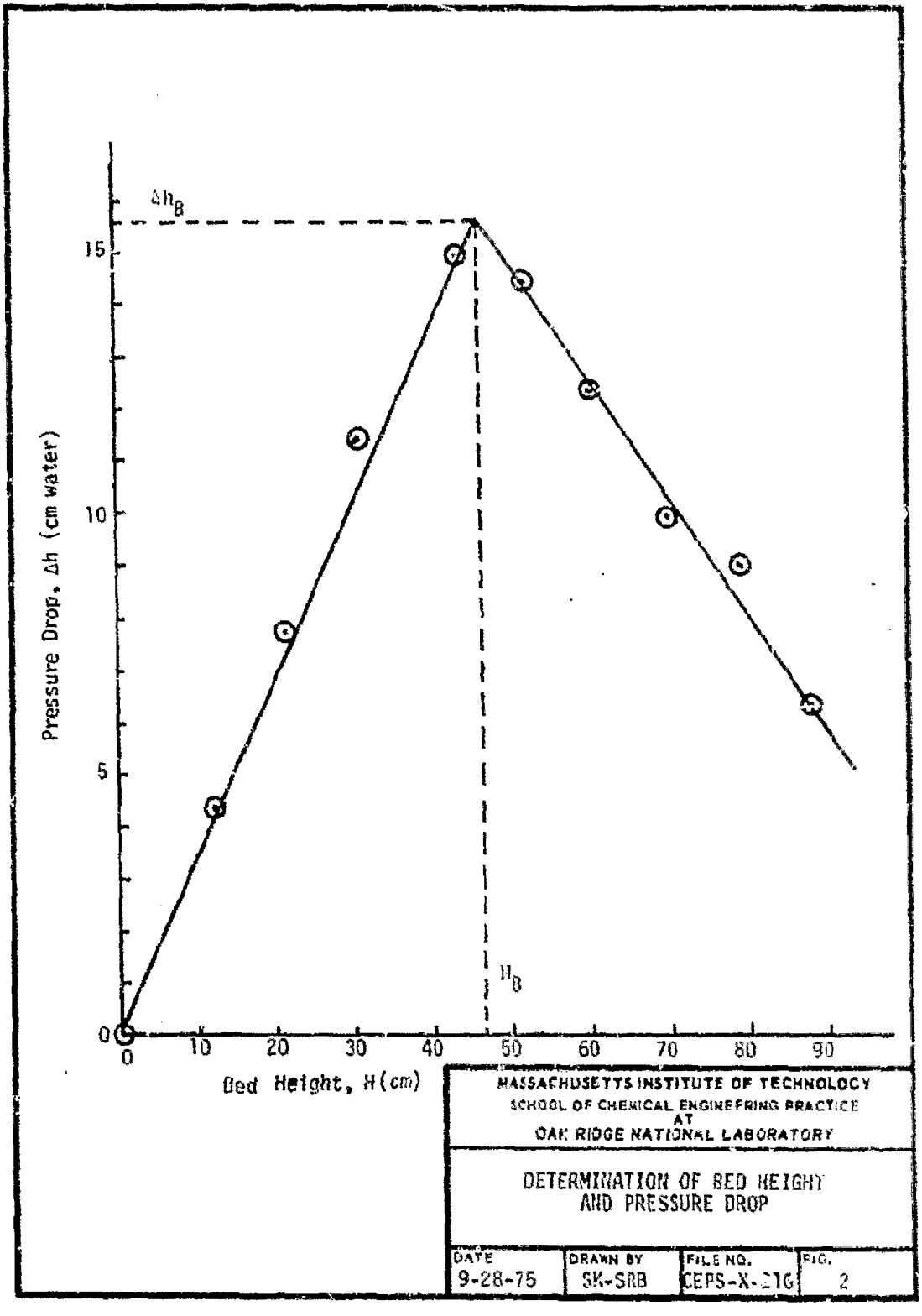
Δh_B
15
10
5
0
Pressure Drop, Δh (cm water)
H_B
0
10
20
30
40
50
60
70
80
90
Bed Height, H(cm)
MASSACHUSETTS INSTITUTE OF TECHNOLOGY
SCHOOL OF CHEMICAL ENGINEERING PRACTICE
AT
OAK RIDGE NATIONAL LABORATORY
DETERMINATION OF BED HEIGHT
AND PRESSURE DROP
DATE
9-28-75
DRAWN BY
SK-SRB
FILE NO.
CEPS-X-216
FIG.
2

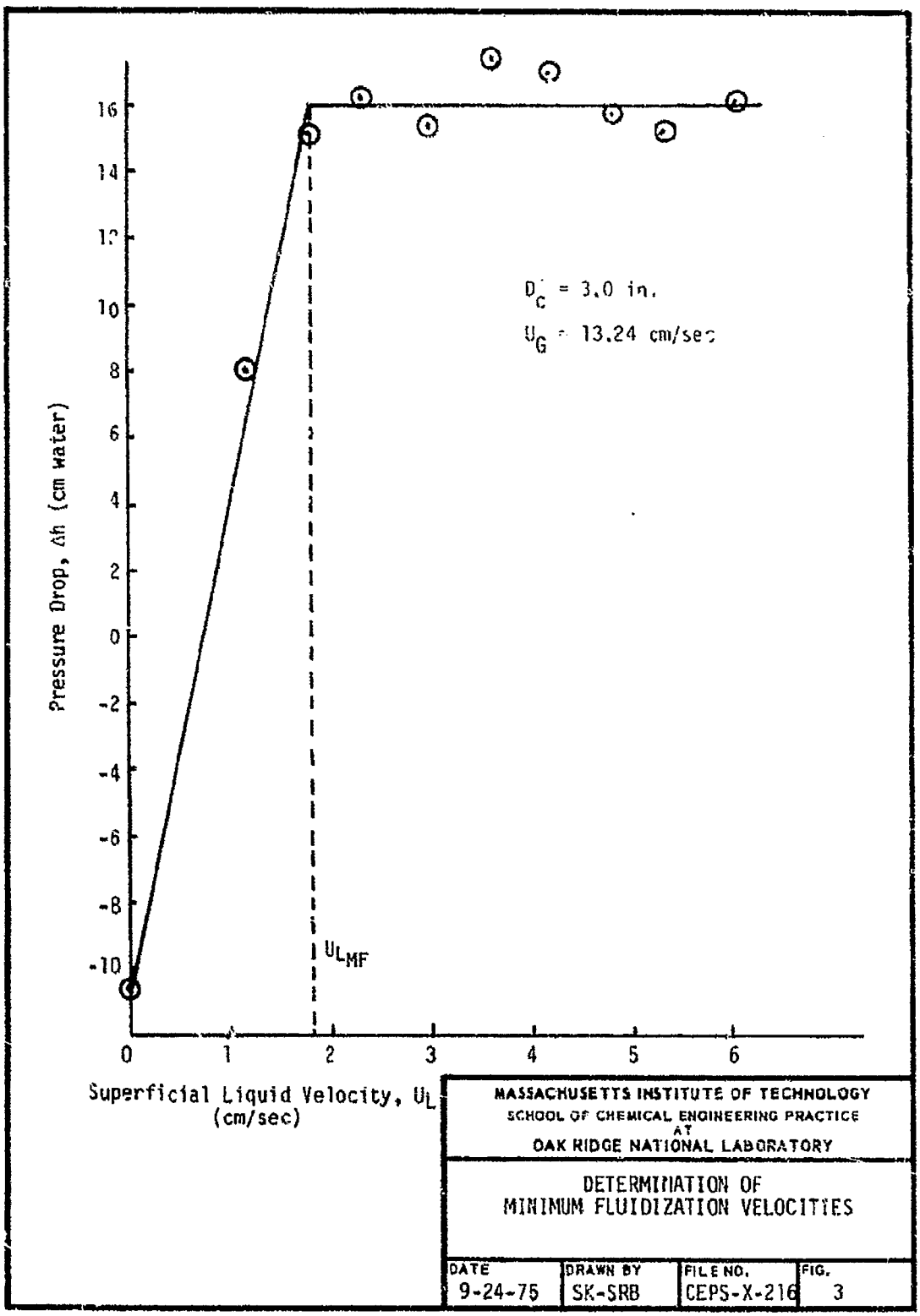
Pressure Drop, Δh (cm water)
16
14
12
10
8
6
4
2
0
-2
-4
-6
-8
-10
D_c = 3.0 in.
U_G = 13.24 cm/sec
$U_{L_{MF}}$
0
1
2
3
4
5
6
Superficial Liquid Velocity, U_L (cm/sec)
MASSACHUSETTS INSTITUTE OF TECHNOLOGY
SCHOOL OF CHEMICAL ENGINEERING PRACTICE
AT
OAK RIDGE NATIONAL LABORATORY
DETERMINATION OF
MINIMUM FLUIDIZATION VELOCITIES
DATE 9-24-75
DRAWN BY SK-SRB
FILE NO. CEPS-X-216
FIG. 3

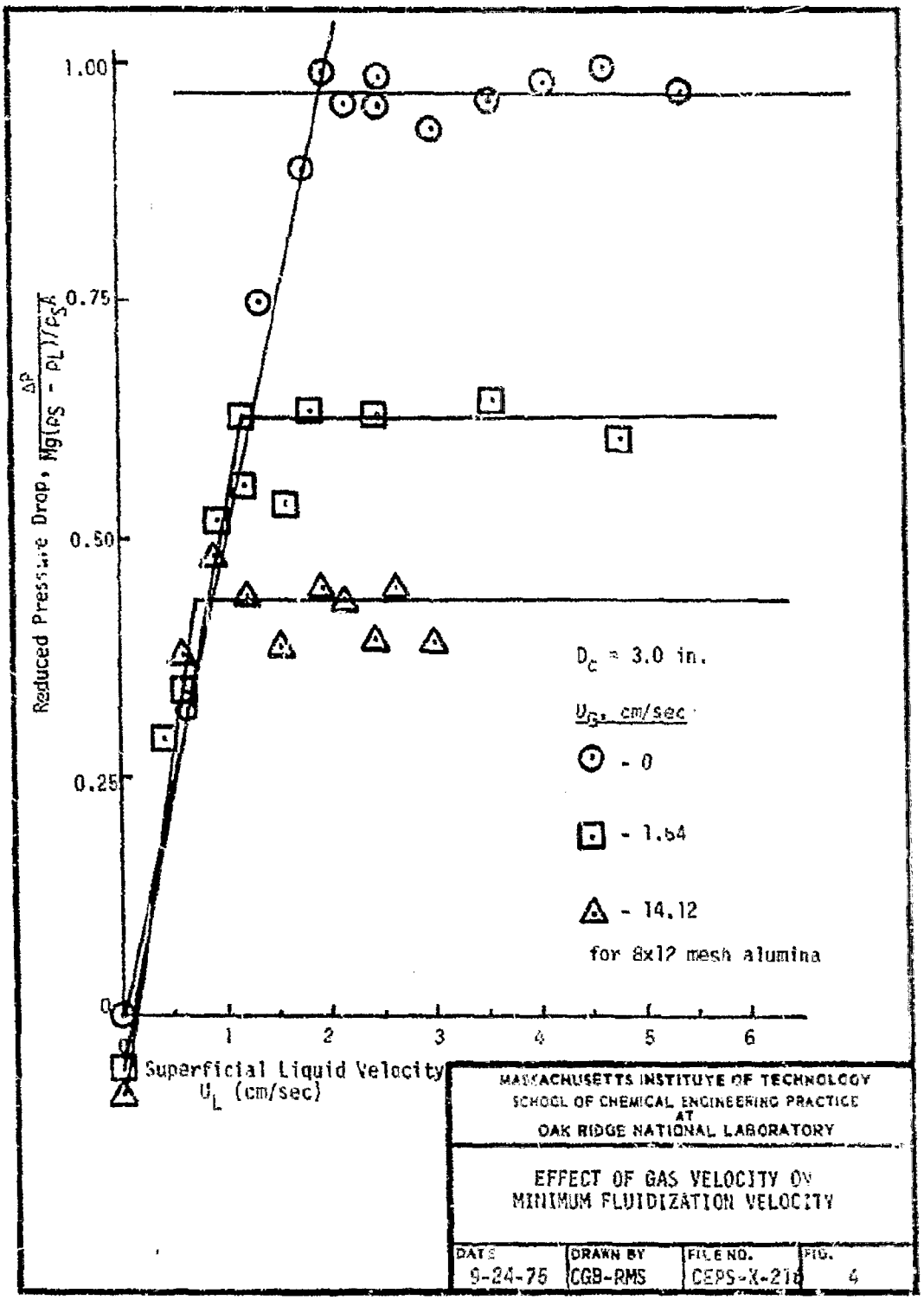
1.00
0.75
0.50
0.25
0
Reduced Pressure Drop, $\frac{\Delta P}{Mg(\rho_S - \rho_L)/\rho_S A}$
1
2
3
4
5
6
Superficial Liquid Velocity
U_L (cm/sec)
D_c = 3.0 in.
U_G, cm/sec
⊙ - 0
⊡ - 1.64
△ - 14.12
for 8x12 mesh alumina
MASSACHUSETTS INSTITUTE OF TECHNOLOGY
SCHOOL OF CHEMICAL ENGINEERING PRACTICE
AT
OAK RIDGE NATIONAL LABORATORY
EFFECT OF GAS VELOCITY ON
MINIMUM FLUIDIZATION VELOCITY
DATE 9-24-75
DRAWN BY CGB-RMS
FILE NO. CEPS-X-218
FIG. 4

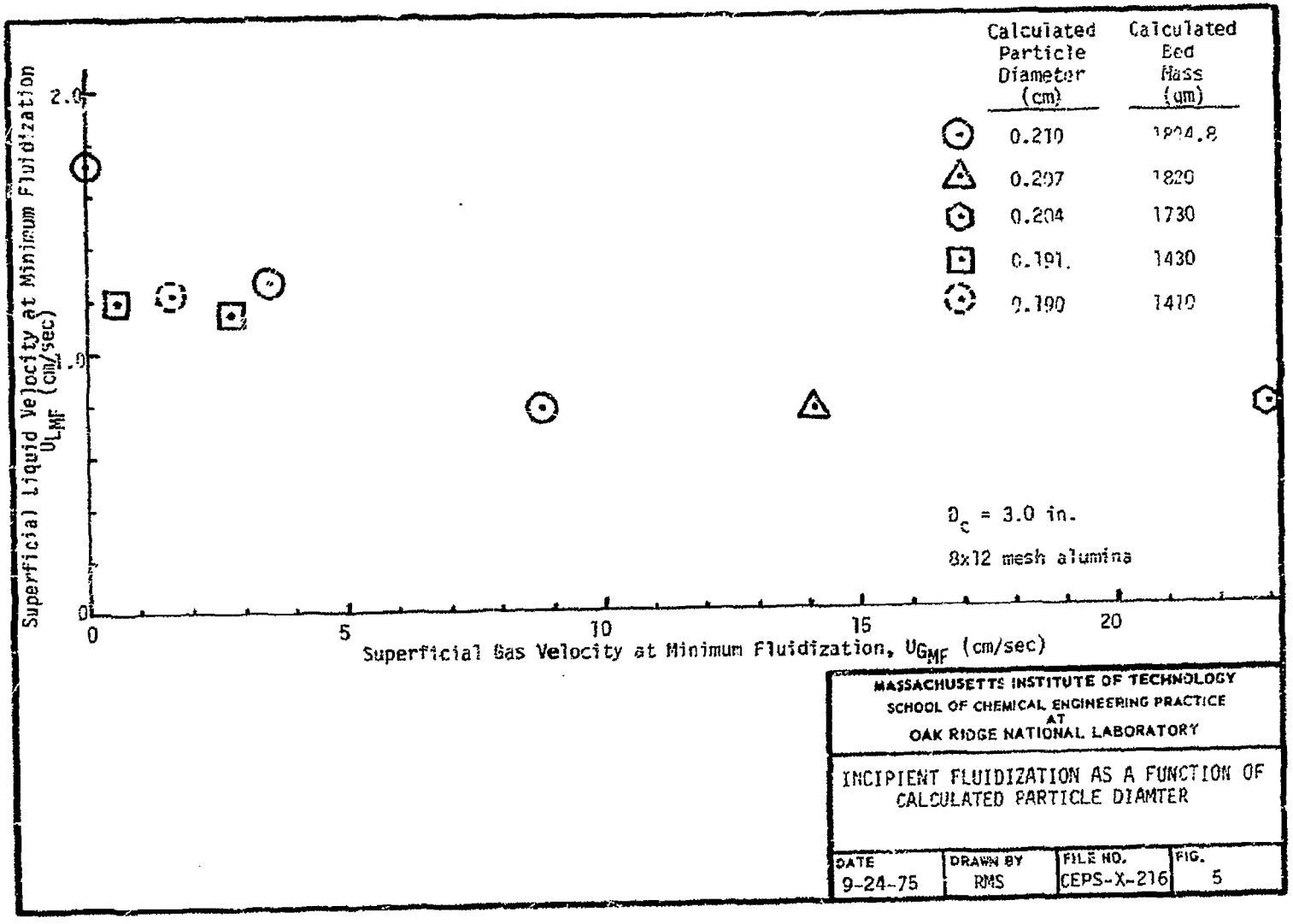
Calculated Particle Diameter (cm)
Calculated Bed Mass (gm)
0.210
1804.8
0.207
1820
0.204
1730
0.191
1430
0.190
1410
D_c = 3.0 in.
8x12 mesh alumina
Superficial Liquid Velocity at Minimum Fluidization $U_{L_{MF}}$ (cm/sec)
Superficial Gas Velocity at Minimum Fluidization, $U_{G_{MF}}$ (cm/sec)
0
5
10
15
20
2.0
1.0
0
MASSACHUSETTS INSTITUTE OF TECHNOLOGY
SCHOOL OF CHEMICAL ENGINEERING PRACTICE
AT
OAK RIDGE NATIONAL LABORATORY
INCIPIENT FLUIDIZATION AS A FUNCTION OF CALCULATED PARTICLE DIAMTER
DATE 9-24-75
DRAWN BY RMS
FILE NO. CEPS-X-216
FIG. 5

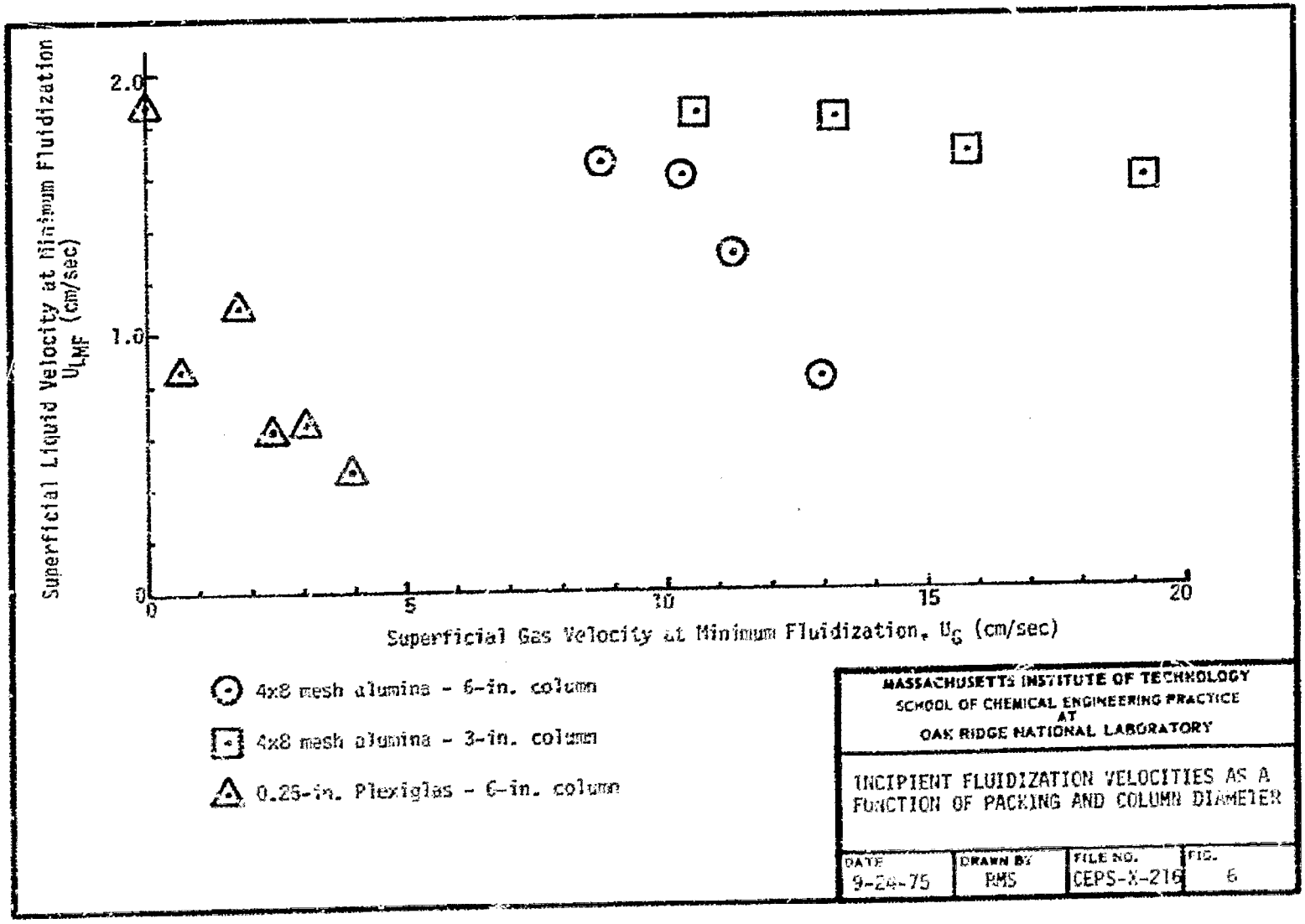
Superficial Liquid Velocity at Minimum Fluidization U_{LMF} (cm/sec)
2.0
1.0
0
0
5
10
15
20
Superficial Gas Velocity at Minimum Fluidization, U_G (cm/sec)
4x8 mesh alumina - 6-in. column
4x8 mesh alumina - 3-in. column
0.25-in. Plexiglas - 6-in. column
MASSACHUSETTS INSTITUTE OF TECHNOLOGY
SCHOOL OF CHEMICAL ENGINEERING PRACTICE
AT
OAK RIDGE NATIONAL LABORATORY
INCIPIENT FLUIDIZATION VELOCITIES AS A FUNCTION OF PACKING AND COLUMN DIAMETER
DATE 9-24-75
DRAWN BY RMS
FILE NO. CEPS-X-216
FIG. 6

dependence of minimum liquid velocities on the large range (0 - 20 cm/sec) of minimum gas velocities for the 8x12 mesh alumina in the 3-in. column is shown in Fig. 5. Attrition losses of the 8x12 mesh alumina occurred especially at high superficial gas velocities. Initially 1894 gm of 8x12 mesh alumina having a mean particle diameter of 0.210 cm were charged to the 3-in. column. During experimentation with this packing, a decrease in static bed height equivalent to a loss of 485 gm of alumina occurred. Particle attrition was noticed by the presence of several hundred grams of solid alumina settled in the liquid storage tanks. The solid bed height for all these experiments with 8x12 mesh alumina were corrected. Since the static bed height was recorded before each run, the change in bed mass was back-calculated by Eq. (14) assuming a constant and independently measured static solid holdup.

$$M = \varepsilon_S^* \rho_S A H_B^* \qquad (14)$$

where * means static conditions.

The decrease in particle diameter was calculated from the calculated bed mass, M, assuming equal attrition of each particle. The calculated mass and particle diameter were then assumed to be constant throughout the run. The calculated particle diameter of the 8x12 mesh alumina removed from the 3-in. column after the last run was 0.191 cm, compared to a measured mean diameter of 0.189 cm. The three gas velocities in the range of 0.55 to 2.7 cm/sec were studied after the most severe attrition had occurred. The particles were smaller by this time and fluidized at lower liquid velocities as is observed in Fig. 5.

A more pronounced dependence of minimum liquid velocities on gas velocities for Plexiglas and 4x8 mesh alumina in the 6-in. column is shown in Fig. 6. Fluidization occurs at lower gas and liquid velocities for the Plexiglas because of its low density difference with water relative to alumina. The insensitivity of minimum liquid fluidization velocities to large gas velocities for 4x8 mesh alumina in the 3-in. column may be due to the transition into a slugging regime. The possibility of slugging in the 3-in. column exists because of large superficial fluid velocities.

4.3 Holdups

4.3.1 Holdups with Alumina Packing

The effects of liquid and gas superficial velocities on solid, liquid, and gas holdups for 8x12 and 4x8 mesh alumina are shown in Figs. 7 through 10. Due to the increase in bed height, the solid holdup decreases with increasing liquid velocities at a constant gas velocity. As the liquid velocity increases, the liquid holdup increases faster than the solid holdup decreases. Since the sum of the holdups must equal one, the result is that the gas holdup decreases slightly with increasing liquid velocities.

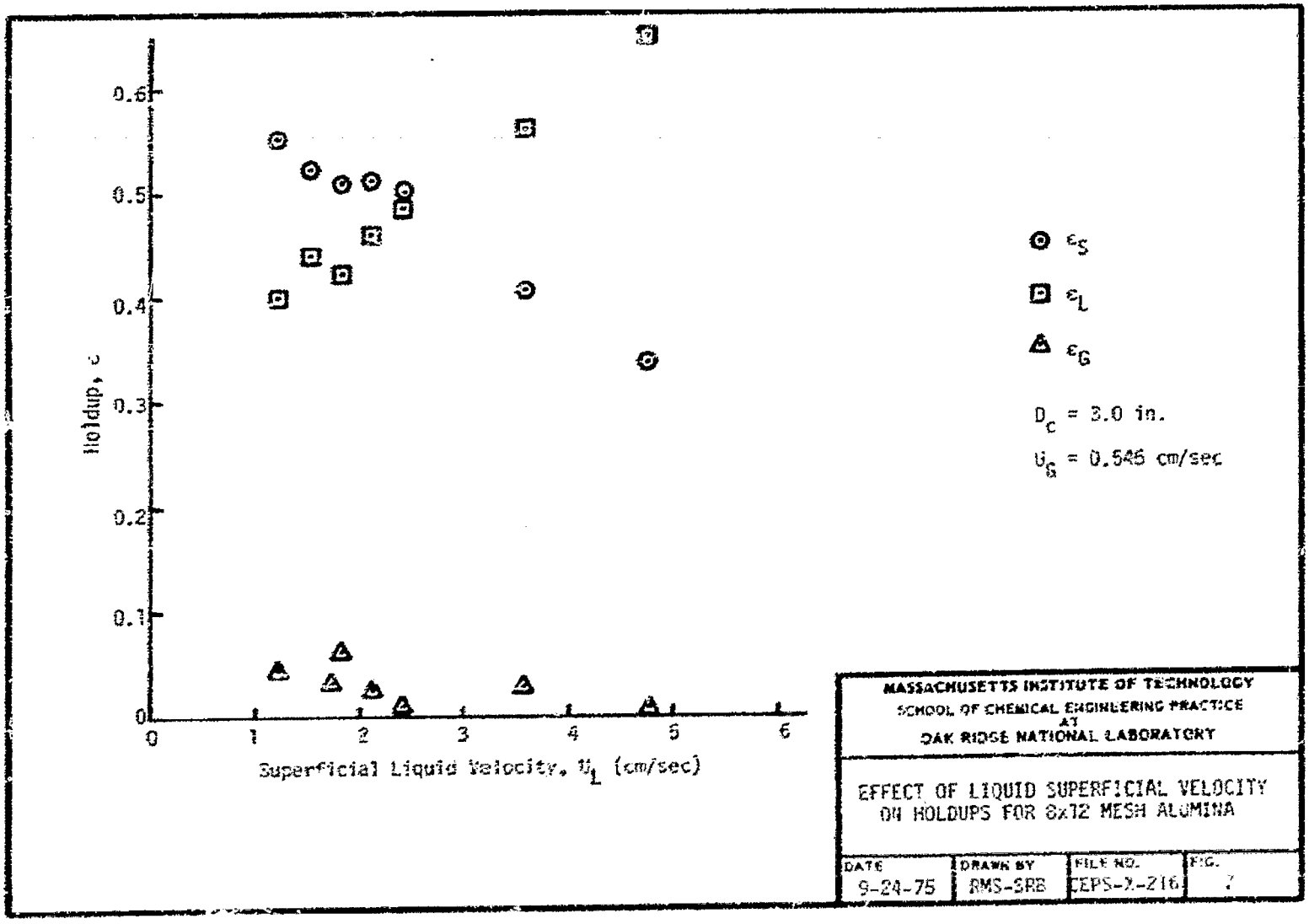
Holdup, ε
0.6
0.5
0.4
0.3
0.2
0.1
0
0
1
2
3
4
5
6
Superficial Liquid Velocity, U_L (cm/sec)
ε_S
ε_L
ε_G
D_c = 3.0 in.
U_G = 0.546 cm/sec
MASSACHUSETTS INSTITUTE OF TECHNOLOGY
SCHOOL OF CHEMICAL ENGINEERING PRACTICE
AT
OAK RIDGE NATIONAL LABORATORY
EFFECT OF LIQUID SUPERFICIAL VELOCITY ON HOLDUPS FOR 8x12 MESH ALUMINA
DATE 9-24-75
DRAWN BY RMS-SRB
FILE NO. CEPS-X-216
FIG. 7

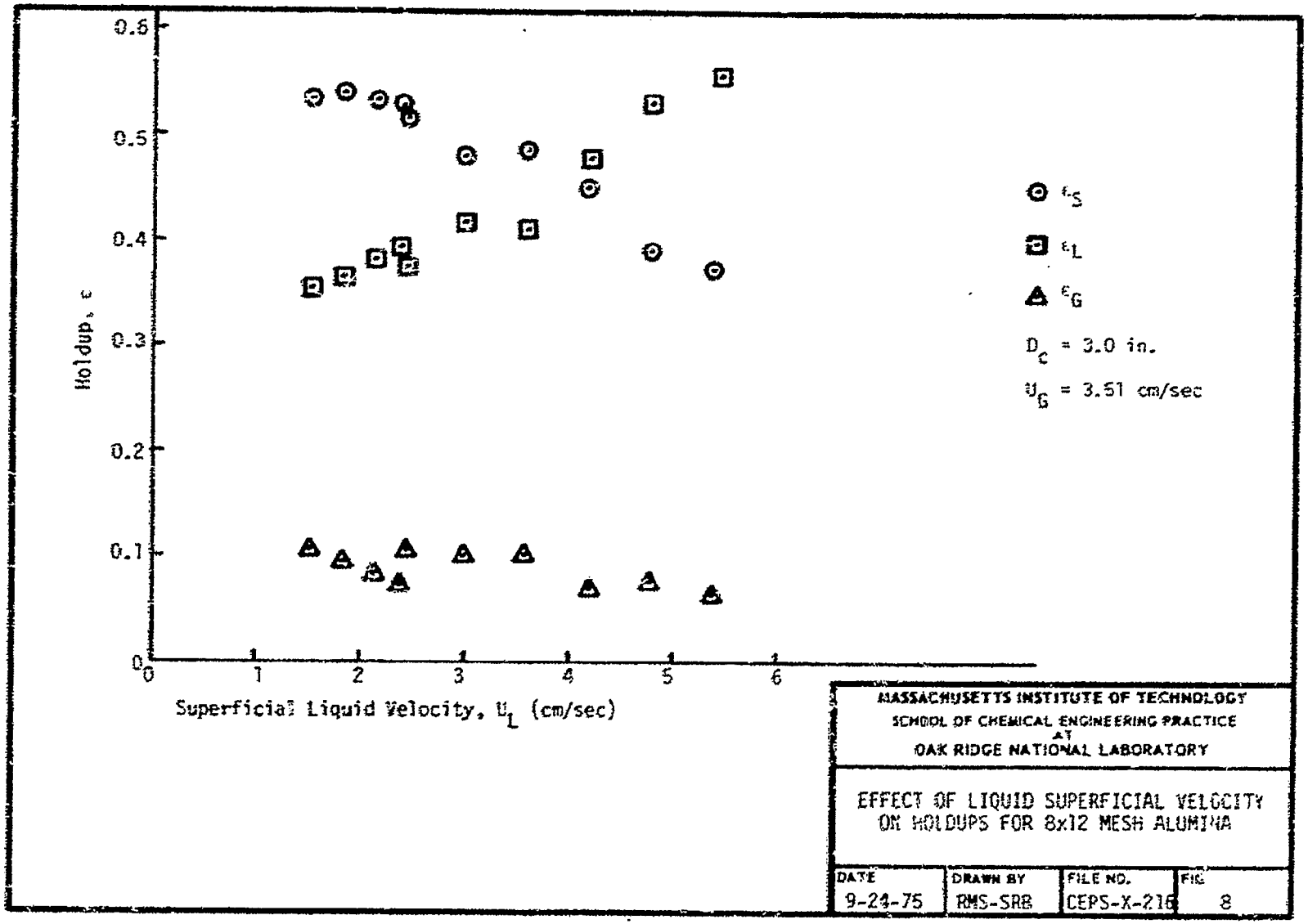
0.6
0.5
0.4
0.3
0.2
0.1
0
Holdup, ε
0
1
2
3
4
5
6
Superficial Liquid Velocity, U_L (cm/sec)
ϵ_S
ϵ_L
ϵ_G
D_c = 3.0 in.
U_G = 3.51 cm/sec
MASSACHUSETTS INSTITUTE OF TECHNOLOGY
SCHOOL OF CHEMICAL ENGINEERING PRACTICE
AT
OAK RIDGE NATIONAL LABORATORY
EFFECT OF LIQUID SUPERFICIAL VELOCITY ON HOLDUPS FOR 8x12 MESH ALUMINA
DATE 9-24-75
DRAWN BY RMS-SRB
FILE NO. CEPS-X-216
FIG. 8

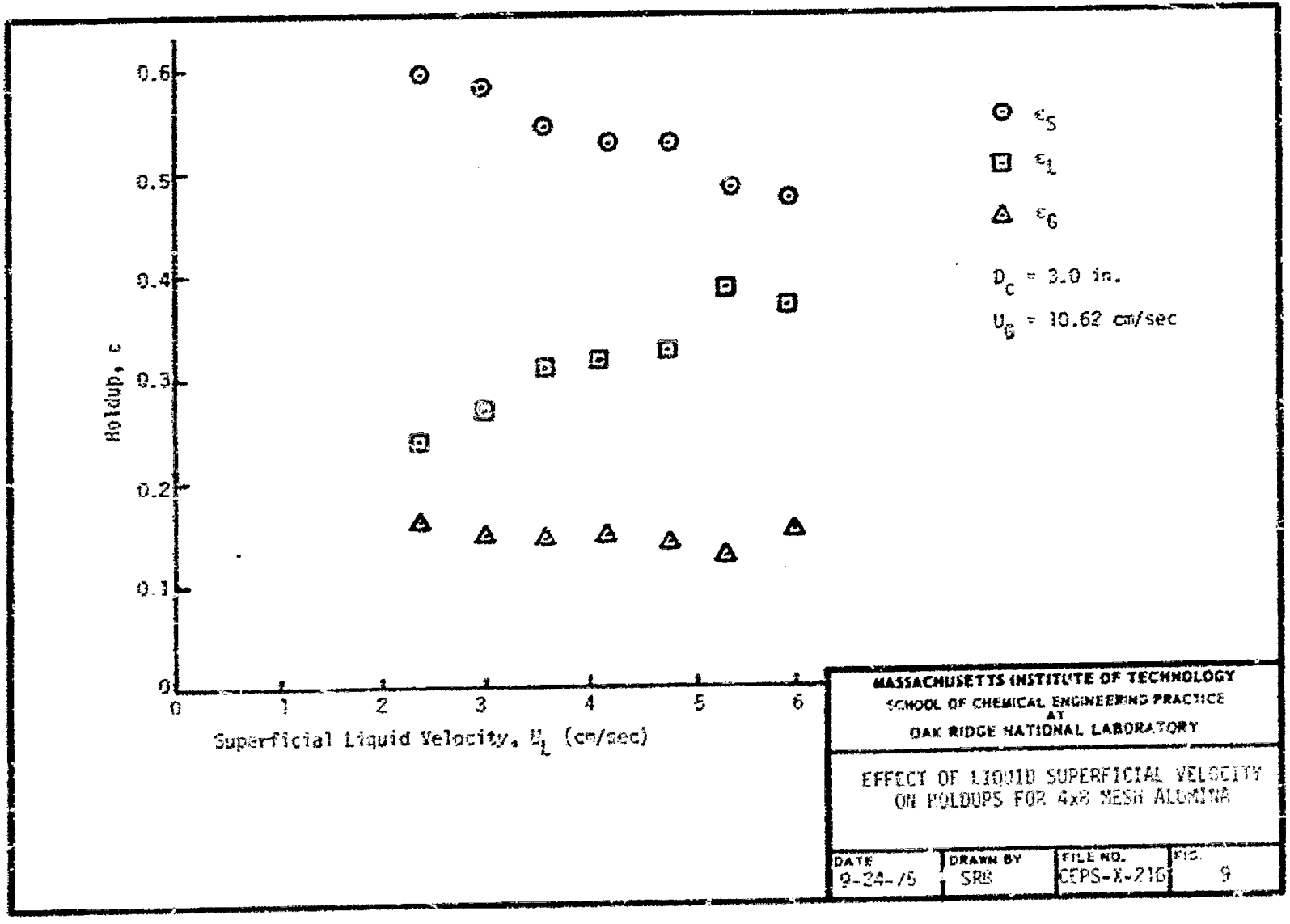
0.6
0.5
0.4
0.3
0.2
0.1
0
Holdup, ε
0
1
2
3
4
5
6
Superficial Liquid Velocity, U_L (cm/sec)
ϵ_S
ϵ_L
ϵ_G
D_C = 3.0 in.
U_G = 10.62 cm/sec
MASSACHUSETTS INSTITUTE OF TECHNOLOGY
SCHOOL OF CHEMICAL ENGINEERING PRACTICE
AT
OAK RIDGE NATIONAL LABORATORY
EFFECT OF LIQUID SUPERFICIAL VELOCITY ON HOLDUPS FOR 4x8 MESH ALUMINA
DATE 9-24-75
DRAWN BY SRB
FILE NO. CEPS-X-216
FIG. 9

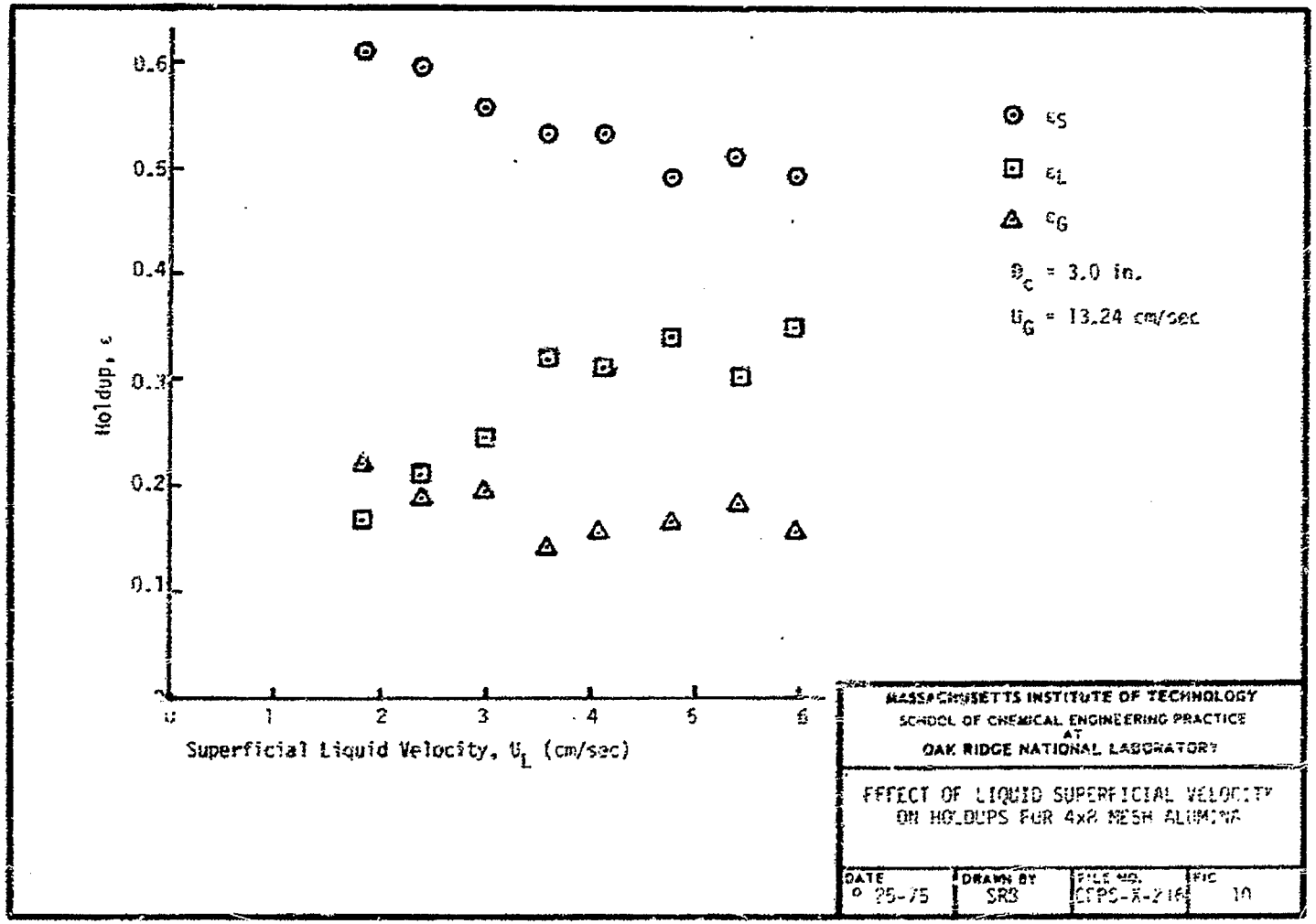
0.6
0.5
0.4
0.3
0.2
0.1
Holdup, ε
0
1
2
3
4
5
6
Superficial Liquid Velocity, U_L (cm/sec)
ε_S
ε_L
ε_G
θ_c = 3.0 in.
U_G = 13.24 cm/sec
MASSACHUSETTS INSTITUTE OF TECHNOLOGY
SCHOOL OF CHEMICAL ENGINEERING PRACTICE
AT
OAK RIDGE NATIONAL LABORATORY
EFFECT OF LIQUID SUPERFICIAL VELOCITY
ON HOLDUPS FOR 4x8 MESH ALUMINA
DATE
9-25-75
DRAWN BY
SRB
FILE NO.
CEPS-A-216
FIG
10

The increase of gas superficial velocity lowers the liquid holdup without an apparent change in the solid holdup.

4.3.2 Holdups with Plexiglas Packing

The solid phase holdup is determined by the application of Eq. (1) assuming the existence of a well-defined bed in which the solid holdup is constant. As the fluid velocities are increased, entrainment of solid particles becomes significant and the holdups vary as a function of axial position in the column. Under these circumstances Eqs. (1) and (3) are no longer applicable. The effect of liquid superficial velocity on the holdups for 0.25-in.-diam Plexiglas is shown in Fig. 11. As liquid velocity increases, the calculated solid and gas holdups increase and the calculated liquid holdup decreases. This is contrary to experimental observation since the bed is visually observed to expand significantly due to the entrainment of the low density Plexiglas spheres at these superficial liquid velocities. The height determined by the intersection of the ΔP-H curves is the bed height of the non-entrained particles. This calculated height decreases with increasing liquid velocity as more particles become entrained above the bed. Equation (1) cannot be applied to solve for the solid holdup when this entrainment occurs. Another method of determining the solid holdup as a function of position in the column was attempted. Plexiglas packing in the ratio of one black to nine clear particles was fluidized at entrainment velocities. Several photographs were taken in an attempt to count the particles as a function of distance up the column. Visual counting was possible in the low particle density region. Unfortunately the number counted for different photographs of the same region at the same conditions varied by more than a factor of two. The number of photographs taken was not sufficient to provide a good statistical average particle density for each region. To enable a statistically valid count in the low particle density regions, the best packing ratio of black to clear Plexiglas beads has to be determined. Once the number of particles in the low density region is known, the particle count in the high density region may be obtained by difference.

4.4 Correlations

4.4.1 Solid Holdup

The solid holdups were correlated by a multivariable linear regression program choosing the same dimensionless groups as Eq. (4). Equation (15) correlates the experimental data and Eq. (16) correlates the experimental and literature data.

$$1 - \epsilon_S = 0.636\ Ca_G^{-0.018}\ Fr_L^{0.107} \qquad (15)$$

where the regression coefficient is 0.87.

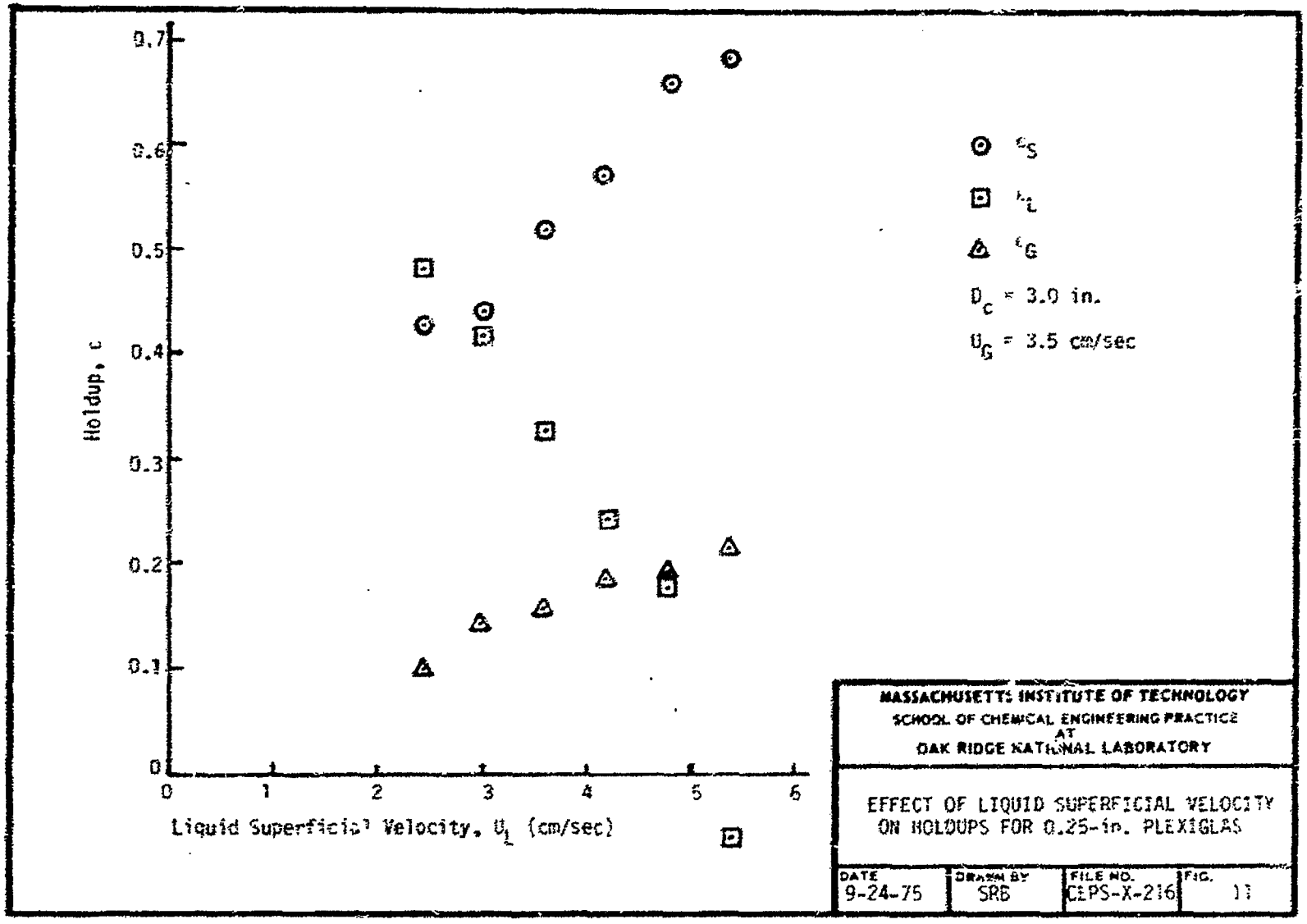

MASSACHUSETTS INSTITUTE OF TECHNOLOGY
SCHOOL OF CHEMICAL ENGINEERING PRACTICE
AT
OAK RIDGE NATIONAL LABORATORY

EFFECT OF LIQUID SUPERFICIAL VELOCITY ON HOLDUPS FOR 0.25-in. PLEXIGLAS

DATE	DRAWN BY	FILE NO.	FIG.
9-24-75	SRB	CEPS-X-216	11

$$1 - \varepsilon_S = 0.596\ Ca_G^{-0.0059\pm0.0042}\ Fr_L^{0.069\pm0.006} \qquad (16)$$

where the regression coefficient is 0.44. The exponents for Eq. (15) are not in agreement with those of Eq. (4). The deviation can be seen in Fig. 12 where the experimental values for solid holdup are plotted against the values of solid holdup calculated by Eq. (4). The experimental data consistently fall below the calculated values. A possible explanation is that Eq. (4) is only valid when no bed contraction is observed. The discrepancy between the correlations result from correlating data for both expanding and contracting beds in a single equation [Eq. (16)]. Equations (4), (15), and (16) are not valid for the two phase solid-liquid fluidization where all predict a solid holdup of unity. In Fig. 13 the experimental values of solid holdup are plotted against holdups calculated from Eq. (16).

Equation (4) was altered by replacing the capillary and Froude numbers by the Reynolds and Archimedes numbers for liquid. A much better correlation was obtained for all data points:

$$1 - \varepsilon_S = 1.17\ Re_L^{0.231\pm0.009}\ Ar_L^{-0.157\pm0.005} \qquad (17)$$

where the regression coefficient is 0.82. Figure 14 shows the experimental data plotted against the calculated holdup from Eq. (17). The data are scattered more evenly about the diagonal indicating a better correlation than previous ones.

The form of Eq. (4) was modified so that the correlation would approach the known limiting value of bed porosity from Eq. (12) as gas velocity approached zero:

$$1 - \varepsilon_S = \left[\frac{18\ Re_L + 2.7\ Re_L^{1.687}}{Ar_L}\right]^{-0.213} \pm a Ca_G^b\ Fr_L^c \qquad (18)$$

Attempts to calculate the coefficients for this correlation failed since when the first term on the right hand side of Eq. (18) is transferred to the left side, the result is a negative number for a portion of the data. As the logarithm of negative numbers is not defined, the multivariable linear regression technique could not be employed to determine the constants a, b, and c.

4.4.2 Liquid Holdup

The liquid holdup was correlated with an equation in the form of Eq. (7). The resulting exponents were not in agreement with the correlation exponents presented by Kim; very small statistical T values were obtained

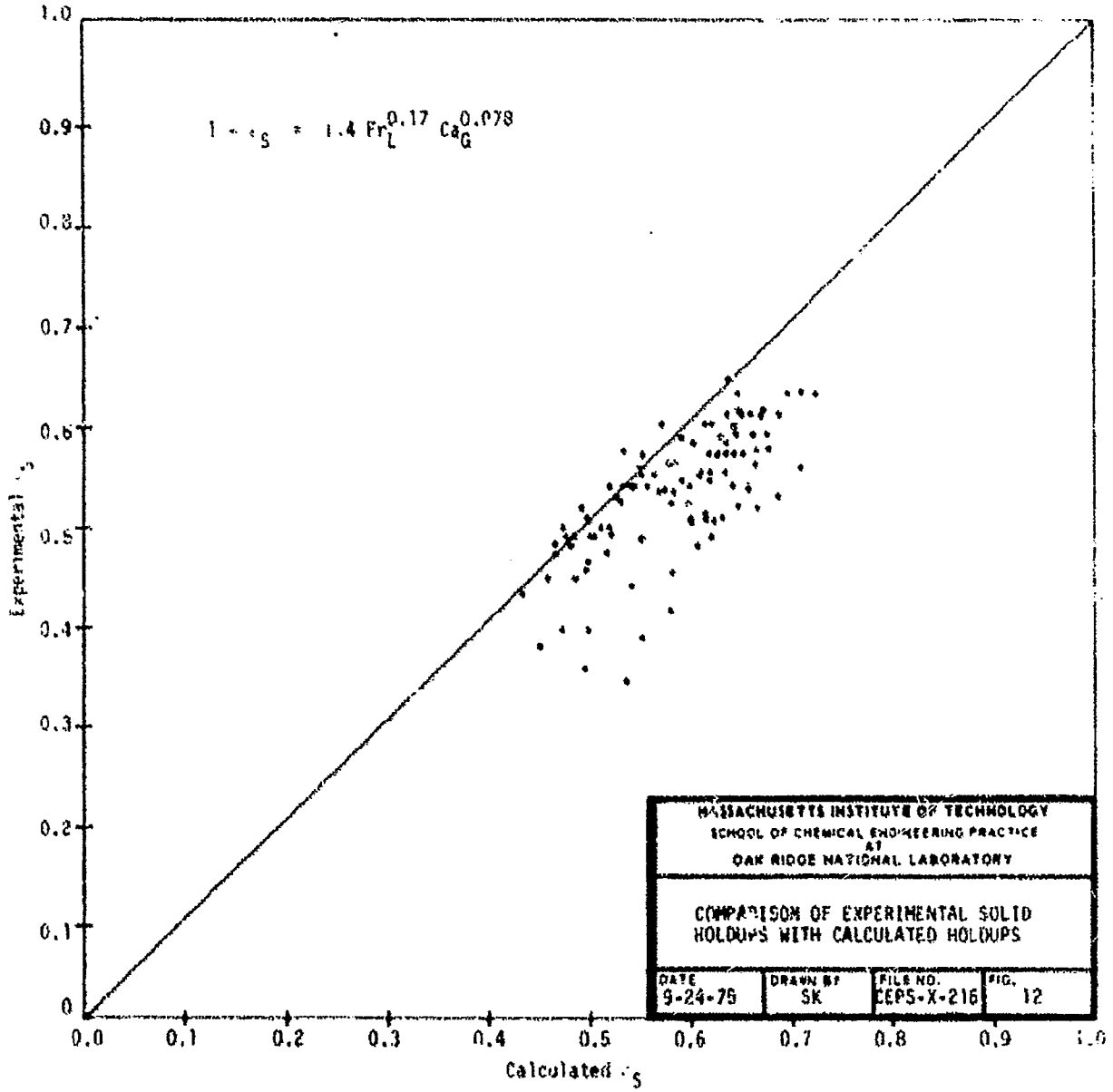
$1 - \epsilon_S = 1.4\ Fr_L^{0.17}\ Ca_G^{0.078}$
Experimental $1-\epsilon_S$
Calculated $1-\epsilon_S$
0.0
0.1
0.2
0.3
0.4
0.5
0.6
0.7
0.8
0.9
1.0
MASSACHUSETTS INSTITUTE OF TECHNOLOGY
SCHOOL OF CHEMICAL ENGINEERING PRACTICE
AT
OAK RIDGE NATIONAL LABORATORY
COMPARISON OF EXPERIMENTAL SOLID HOLDUPS WITH CALCULATED HOLDUPS
DATE 9-24-75
DRAWN BY SK
FILE NO. CEPS-X-216
FIG. 12

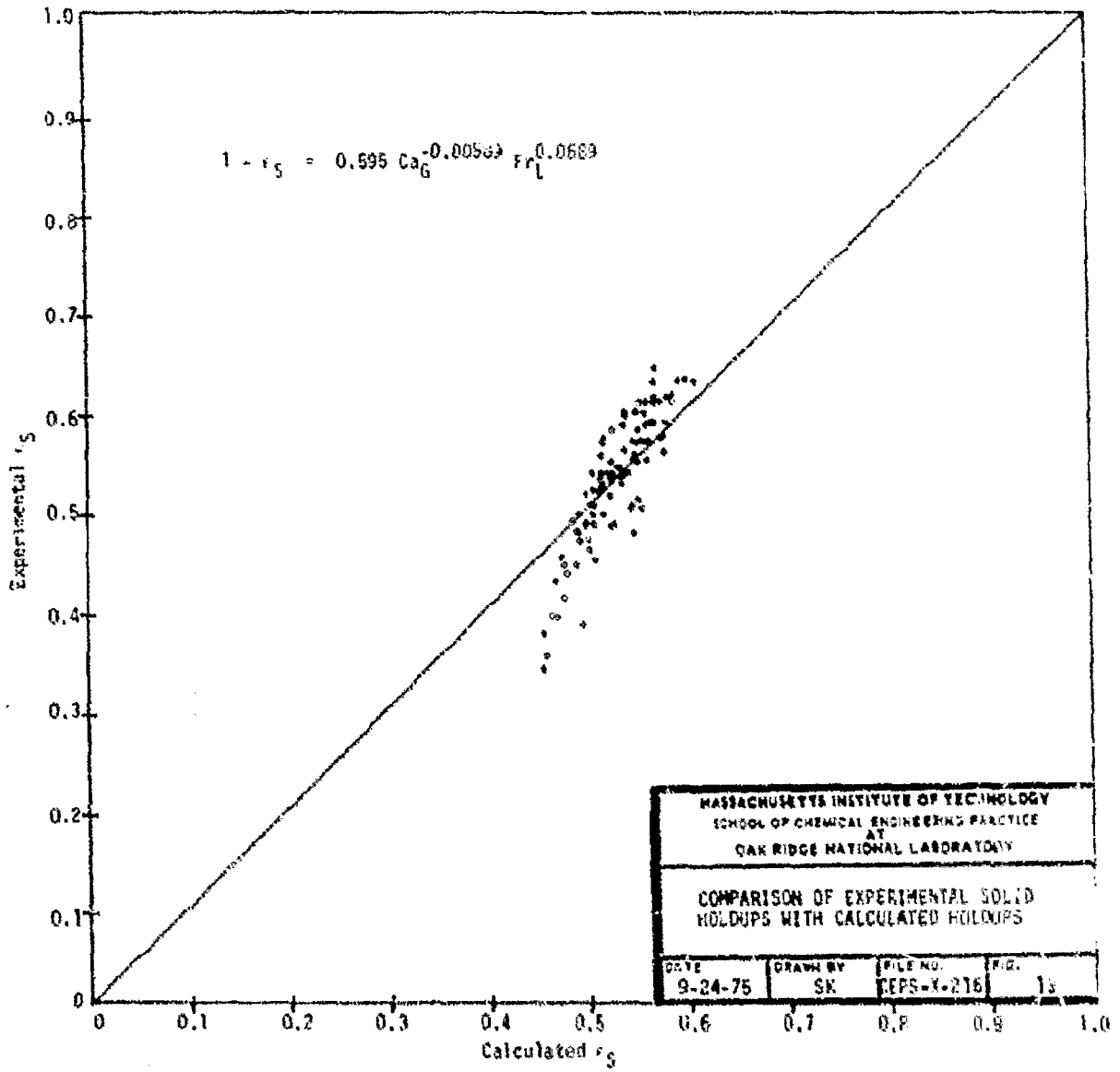
$1 - \epsilon_S = 0.595\ Ca_G^{-0.0056}\ Fr_L^{0.0689}$
Experimental ϵ_S
Calculated ϵ_S
0
0.1
0.2
0.3
0.4
0.5
0.6
0.7
0.8
0.9
1.0
MASSACHUSETTS INSTITUTE OF TECHNOLOGY
SCHOOL OF CHEMICAL ENGINEERING PRACTICE
AT
OAK RIDGE NATIONAL LABORATORY
COMPARISON OF EXPERIMENTAL SOLID HOLDUPS WITH CALCULATED HOLDUPS
DATE 9-24-75
DRAWN BY SK
FILE NO. CEPS-X-216
FIG. 1a

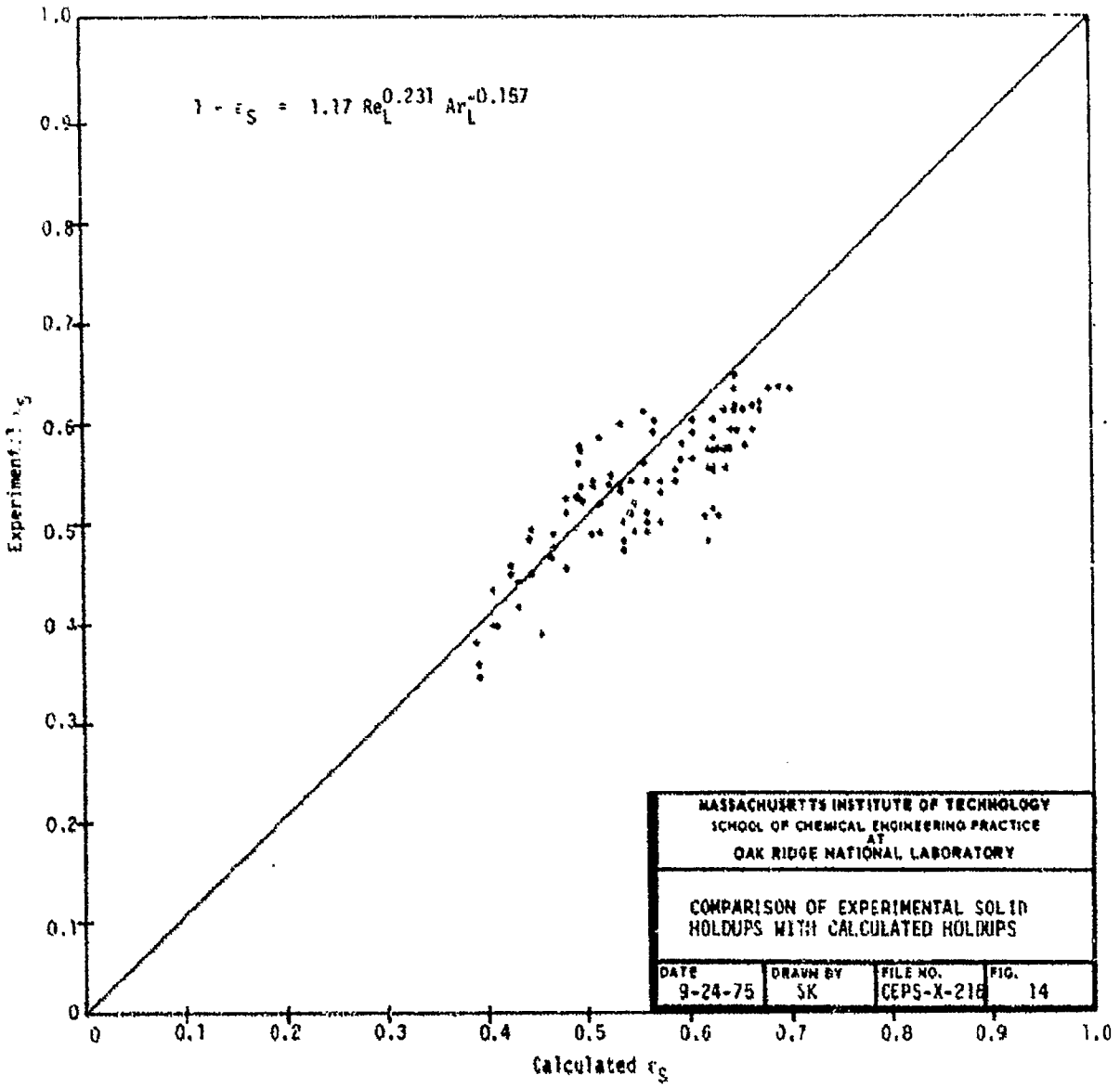
$1 - \varepsilon_S = 1.17\ Re_L^{0.231}\ Ar_L^{-0.157}$
Experimental $1-\varepsilon_S$
Calculated $1-\varepsilon_S$
0
0.1
0.2
0.3
0.4
0.5
0.6
0.7
0.8
0.9
1.0
MASSACHUSETTS INSTITUTE OF TECHNOLOGY
SCHOOL OF CHEMICAL ENGINEERING PRACTICE
AT
OAK RIDGE NATIONAL LABORATORY
COMPARISON OF EXPERIMENTAL SOLID HOLDUPS WITH CALCULATED HOLDUPS
DATE 9-24-75
DRAWN BY SK
FILE NO. CEPS-X-218
FIG. 14

for each of the correlated variables. A comparison of the experimental liquid holdups and holdups calculated by Eq. (7) is shown in Fig. 15. The experimental liquid holdups fall above and below the calculated holdups crossing the diagonal.

A second correlation of the form:

$$\varepsilon_L = \left[\frac{18\ Re_L + 2.7\ Re_L^{1.687}}{Ar_L}\right]^{-0.213} + a Ca_G^b\ Fr_L^c\ Fr_G^d\ Re_L^e \qquad (19)$$

was attempted. As in the previous correlation, the statistical T values for the exponents were very small and a significant correlation was not obtained.

4.4.3 Gas Holdup

A correlation for gas holdup of the form

$$\varepsilon_G = 0.322\left[\frac{\rho_L U_G^4}{g\sigma}\right]^{0.219} \pm a Ca_G^b\ Fr_L^c\ F_G^d\ Re_L^e \qquad (20)$$

was attempted. As in the case of solid holdup, the transfer of the first term on the right side of Eq. (20) to the left side often yields negative numbers and therefore the multivariable linear regression technique could not be applied.

5. CONCLUSIONS

1. The following correlations were obtained for the solid holdup using all the data available:

$$1 - \varepsilon_S = 0.596\ Ca_G^{-0.0059\pm0.0042}\ Fr_L^{0.069\pm0.006}$$

$$1 - \varepsilon_S = 1.17\ Re_L^{0.231\pm0.009}\ Ar_L^{-0.157\pm0.005}$$

2. Solid holdup can be measured by the pressure drop technique only if there exists a definite bed height.

3. As previously reported, the three-phase minimum liquid fluidization velocity decreases with increasing gas velocity over the range studied.

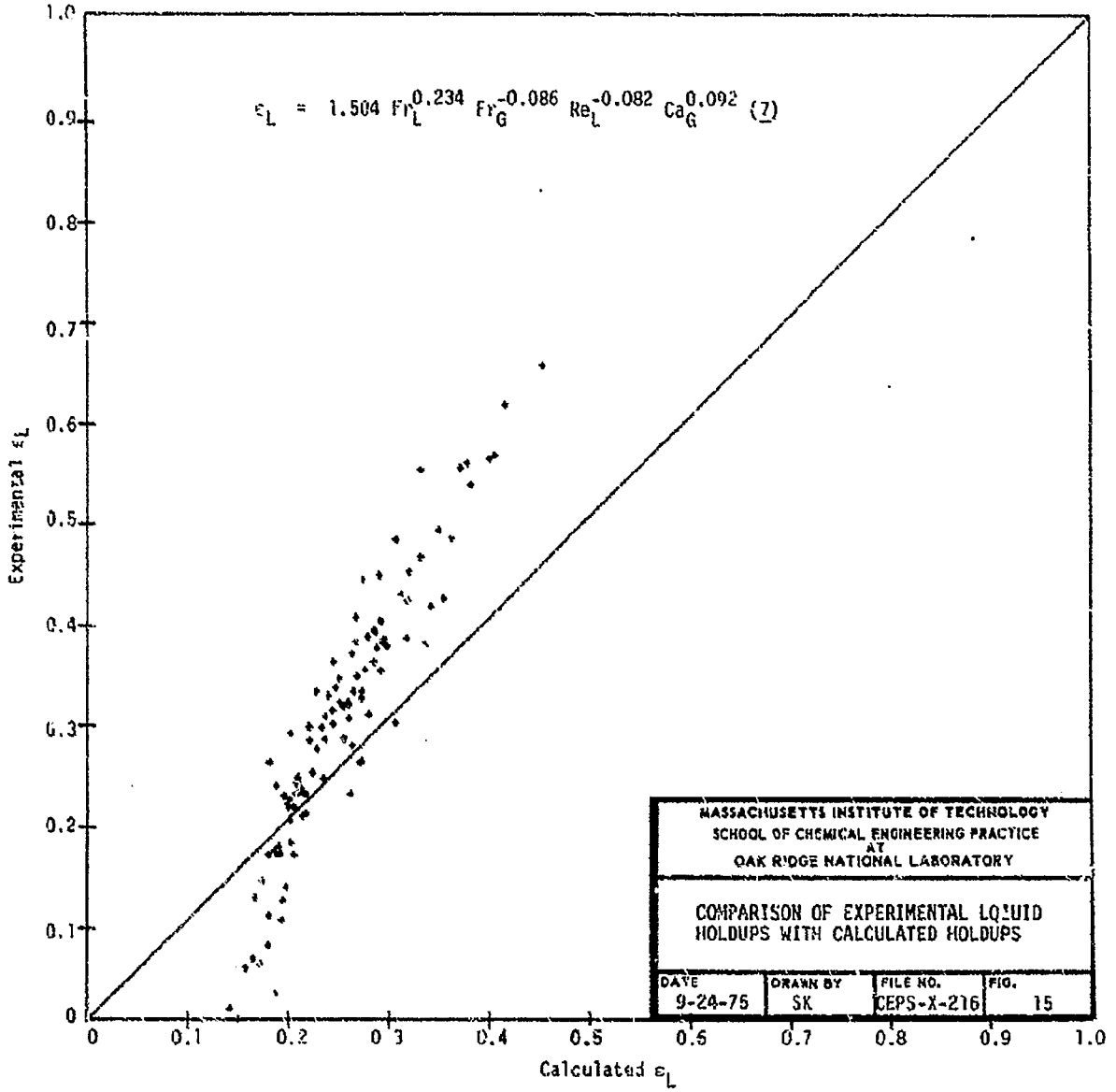
$\varepsilon_L = 1.504\ Fr_L^{0.234}\ Fr_G^{-0.086}\ Re_L^{-0.082}\ Ca_G^{0.092}$ (7)
Experimental ε_L
Calculated ε_L
0
0.1
0.2
0.3
0.4
0.5
0.6
0.7
0.8
0.9
1.0
MASSACHUSETTS INSTITUTE OF TECHNOLOGY
SCHOOL OF CHEMICAL ENGINEERING PRACTICE
AT
OAK RIDGE NATIONAL LABORATORY
COMPARISON OF EXPERIMENTAL LIQUID HOLDUPS WITH CALCULATED HOLDUPS
DATE 9-24-75
DRAWN BY SK
FILE NO. CEPS-X-216
FIG. 15

The solid holdup decreases as the liquid velocity is increased. The gas holdup decreases as the liquid velocity is increased.

4. Attrition of 8x12 mesh alumina particles in a three-phase fluidized bed is significant at high gas flow rates.

6. RECOMMENDATIONS

1. Develop photographic technique to measure ϵ_S in the region of undefined bed height by determining the number of pictures necessary for a statistical time average in the region, the optimum black-to-clear bead ratio, and the maximum allowable column diameter.

2. Improve accuracy of the pressure drop measurement along the column by decreasing the diameter of the column-to-manometer connecting lines to dampen oscillations at high gas velocities and to prevent the small alumina from clogging the lines. A continuous pressure profile could be obtained using a single moveable J-shaped manometer inside the column, small enough not to disrupt the flow pattern.

3. Increase the operating ranges of the system by using larger pumps, removing the gas regulator, increasing the column height, and increasing the size of the syphon breaker tube for faster overflow in the 3-in. column.

4. Use smaller, more abrasion resistant and constant diameter packing such as glass marbles, plastics, or ball bearings.

7. ACKNOWLEDGMENT

The authors wish to thank J.M. Begovich and J.S. Watson for their help during the project.

8. APPENDIX

8.1 Derivation of Holdup Formulas

The holdup of any particular phase is defined as the volume fraction of that phase in the bed. This definition is written for the general case as

$$\varepsilon_i = V_i/V_B \tag{21}$$

For the solids holdup, the volume of solids may be written as

$$V_S = M_S/\rho_S \tag{22}$$

The volume of the bed may be written as

$$V_B = AH_B \tag{23}$$

Substituting Eqs. (22) and (23) into Eq. (21) yields

$$\varepsilon_S = \frac{M}{\rho_S A H_B} \tag{1}$$

In Eq. (1) the mass and density of solids and the column area are known, and the bed height is determined by the pressure profile in the column as shown in Fig. 2.

The equations for the liquid and gas holdups are derived from the bed height and pressure drop across the bed. The pressure drop across any segment of the column is equal to the total weight of the material in that segment. The pressure drop may be represented by

$$\Delta P = \rho_B g H_B \tag{24}$$

where the density is the weighted density of the material in the segment. This weighted density may be written in terms of the holdups:

$$\rho_B = \varepsilon_S\rho_S + \varepsilon_L\rho_L + \varepsilon_G\rho_G \tag{25}$$

This equation may be substituted into Eq. (24) to yield

$$\Delta P = (\varepsilon_S \rho_S + \varepsilon_L \rho_L + \varepsilon_G \rho_G) g H_B \tag{3}$$

The sum of the holdups must equal one

$$1 = \varepsilon_S + \varepsilon_G + \varepsilon_L \tag{2}$$

Equations (2) and (3) are solved simultaneously to yield

$$\varepsilon_G = \frac{\frac{\Delta P}{g H_B} - \varepsilon_S \rho_S - \rho_L + \varepsilon_S \rho_L}{\rho_G - \rho_L} \tag{26}$$

and

$$\varepsilon_L = 1 - \varepsilon_S - \varepsilon_G \tag{27}$$

The pressure drop in the above formulas was measured by the water manometers located along the column. As shown in Fig. 16, the pressure at the top of the bed was measured by

$$P_B - P_{atm} = \rho_L g H_{m_B} \tag{28}$$

The pressure drop at the bottom of the bed was measured by

$$P_o - P_{atm} = \rho_L g H_{m_o} \tag{29}$$

The height of the bottom manometer may be rewritten as

$$H_{m_o} = H_B + H_{m_B} + \Delta h \tag{30}$$

Substituting Eq. (30) into Eqs. (24), (28), and (29), the pressure drop across the bed was found by

$$\Delta P = P_o - P_B = \rho_L g (H_B + \Delta h) \tag{31}$$

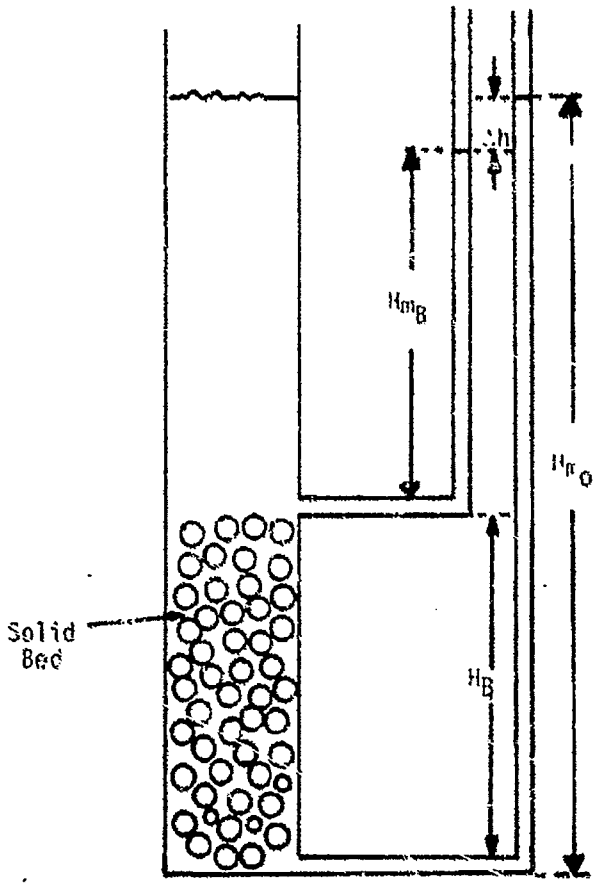

MASSACHUSETTS INSTITUTE OF TECHNOLOGY SCHOOL OF CHEMICAL ENGINEERING PRACTICE AT OAK RIDGE NATIONAL LABORATORY			
PRESSURE DROP DETERMINATION			
DATE 9-24-75	DRAWN BY SK-SRB	FILE NO. CEPS-X-216	FIG. 16

Substituting this pressure drop into Eq. (26), the gas holdup is found by

$$\varepsilon_G = \frac{\frac{H_B + \Delta h}{H_B}\rho_L - \varepsilon_S\rho_S - \rho_L + \varepsilon_S\rho_L}{\rho_G - \rho_L} \qquad (32)$$

and the liquid holdup was found by substituting for ε_G in Eq. (27).

8.2 Sample Calculations

Sample calculations are shown for Run 31 (ORNL Databook A-7217-G). The 3-in.-diam column was charged with 2270 gm of 4x8 mesh alumina having a density of 1.94 gm/cm^3 and a 0.357-cm particle diameter. The bottom manometer read 90.7 cm, and the top manometer 68.5 cm at static conditions. A static pressure correction factor of (90.7 - 68.5) or 22.2 cm was determined for the last manometer. At a superficial gas velocity of 13.24 cm/sec and a superficial liquid velocity of 2.98 cm/sec, a height of 84.0 cm was recorded in the bottom manometer and a height of 55.5 cm in the top manometer. Thus, the pressure drop due to flow is

$$\Delta h = 84.0 - (55.5 + 22.2) = 6.3 \text{ cm}$$

The bed height and bed pressure drop is determined by a plot of the Δh readings against the distance up the column. Figure 2 illustrates this procedure for a gas velocity of 13.24 cm/sec and a liquid velocity of 2.98 cm/sec in Run 31. A bed height of 46.0 cm and a pressure drop of 15.3 cm of water were calculated. The pressure drop across the bed was obtained for several liquid flow rates and plotted for Run 31 in Fig. 3. From this plot the minimum fluidization point for the bed in Run 31 is 1.82 cm/sec of water and 13.24 cm/sec of air.

The solid holdup for the fluidized bed in Run 31 at a gas velocity of 13.24 cm and liquid velocity of 2.98 cm was calculated

$$\varepsilon_S = \frac{M}{\rho_S A H_B} = \frac{2270 \text{ gm}}{(1.94 \text{ gm/cm}^3)[(\frac{3 \text{ in.}}{2})(2.54 \frac{\text{cm}}{\text{in.}})]^2\pi(46 \text{ cm})}$$

$$= 0.557$$

The gas holdup was calculated,

$$\varepsilon_G = \frac{\left(\frac{H_B + \Delta h}{H_B}\right)(\rho_L) + \varepsilon_S\rho_S - \rho_L + \varepsilon_S\rho_L}{\rho_G - \rho_L} \qquad (32)$$

$$= \frac{\frac{46+15.3\ cm}{46\ cm}(.995\ \frac{gm}{cm^3}) - 0.557(1.942\ \frac{gm}{cm^3}) - 0.995\ \frac{gm}{cm^3} + (.557)(.995\ \frac{gm}{cm^3})}{0.0012 - 0.995\ gm/cm^3}$$

$$= 0.195$$

The liquid holdup was calculated,

$$\varepsilon_L = 1 - \varepsilon_S - \varepsilon_G = 1 - 0.557 - 0.195 = 0.248 \qquad (27)$$

8.3 Location of Original Data

The original data are located in ORNL Databooks A-7217-G, pp. 17-100, and A-7215-G, pp. 13-23. The databooks and calculations are on file at the MIT School of Chemical Engineering Practice, Bldg. 3001, ORNL.

8.4 Nomenclature

a	correlation constant
A	cross sectional area, cm^2
Ar_L	Archimedes number, liquid phase, $D_p^3\rho_L(\rho_S - \rho_L)g/\mu_L^2$
b	correlation constant
c	correlation constant
Ca_G	capillary number, based on gas velocity, $U_G\mu_L/G_L$
d	correlation constant
D_c	diameter of column, in.
D_p	diameter of packing, cm
e	correlation constant

Fr_i Froude number, based on phase i, U_i^2/gD_p

g gravitational constant, cm/sec^2

H height along column, cm

h incremental manometer height, cm of H_2O

M mass of solids in bed, gm

P pressure, $dyne/cm^2$

Re_L Reynolds number, liquid phase, $U_L D_p \rho_L / \mu_L$

R regression coefficient

U superficial velocity, cm/sec

U_t terminal velocity, cm/sec

V volume, cm^3

Subscripts:

B bed

G gas phase

i i^{th} phase

L liquid phase

m manometer

MF at minimum fluidization

o manometer at bottom of column

p particle

S solid phase

Greek Symbols:

ε holdup (volume fraction)

ρ density, gm/cm^3

σ surface tension, dyne/cm

μ viscosity, gm/cm-sec

8.5 Literature References

1. Burck, G.M., K. Kodama, R.G. Markeloff, and S.R. Wilson, "Cocurrent Three-Phase Fluidized Bed (Part 2)," ORNL-MIT-213 (May 1975).

2. Dakshinamurty, P., V. Subrahmanyam, and J. Rao, "Bed Porosities in Gas-Liquid Fluidization," I&EC Proc. Des. Dev., 10, 322 (1971).

3. Efremov, G.I., and I.A. Vakhrushev, "A Study of the Hydrodynamics of Three-Phase Fluidized Beds," Intern. Chem. Eng., 10(1), 37 (1970).

4. Ferguson, D.E., ed., "Chemical Technology Division Annual Progress Report for the Period Ending March 31, 1974," ORNL-4966.

5. Kim, S.D., C.G.J. Baker, and M.A. Bergougnou, "Holdup and Axial Mixing Characteristics of Two and Three Phase Fluidized Beds," Can. J. Chem. Eng., 50, 695 (1972).

6. Kim, S.D., C.G.J. Baker, and M.A. Bergougnou, "Phase Holdup Characteristics of Three Phase Fluidized Beds," Can. J. Chem. Eng., 53, 134 (1975).

7. Østergaard, K., and M.L. Michelsen, "Holdup and Axial Dispersion in Gas-Liquid Fluidized Beds," Preprint 31D, Symposium on Fundamental and Applied Fluidization, Tampa, May 1968.

8. Wen, C.Y., and Y.H. Yu, "Mechanics of Fluidization," Chem. Eng. Progr. Symposium Ser., 62, 100 (1966).